Nanoscale

Accepted Manuscript

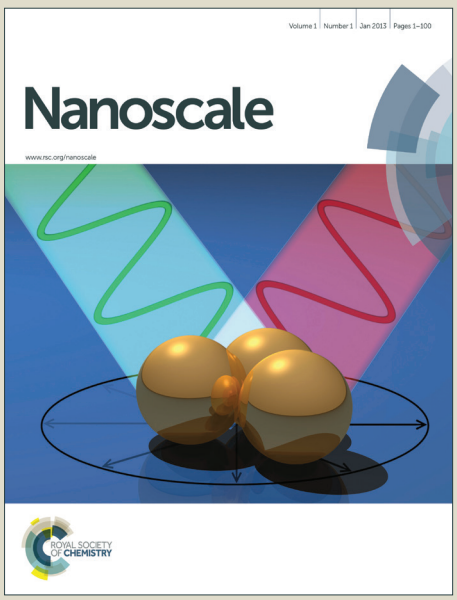

ROYAL SOCIETY OF CHEMISTRY

www.rsc.org/nanoscale

Single-Step Direct Fabrication of Luminescent Cu-doped $Zn_xCd_{1-x}S$ Quantum Dot Thin Films *via* a Molecular Precursor Solution Approach and Their Application in Luminescent, Transparent, and Conductive Thin Films†

Yanyan Chen, Shenjie Li, Lijian Huang, Daocheng Pan*

State Key Laboratory of Rare Earth Resource Utilization, Changchun Institute of Applied Chemistry, Chinese Academy of Sciences, Changchun, Jilin, 130022, China

Tel & Fax: +86-431-85262941; Email: pan@ciac.ac.cn

Abstract

Luminescent Cu-doped $Zn_xCd_{1-x}S$ quantum dot thin films have been directly fabricated *via* a facile solution method in the open air. Cu_2O, ZnO, and $Cd(OH)_2$ were used as the starting materials, and 3-mercaptopropionic acid was used as the capping agents. The effects of Cu dopant concentration, sintering temperature, and sintering time on the photoluminescence properties of Cu-doped $Zn_xCd_{1-x}S$ nanocrystal thin films have been systematically investigated. As-prepared quantum dot thin films exhibit a tunable emission covering the whole visible light region and the absolute photoluminescence quantum yields can reach as high as 25.5%, which have a high potential application in luminescent, transparent, and conductive thin films.

Keywords: Quantum dots; Luminescent thin films; Doped nanocrystals;

TOC Figure

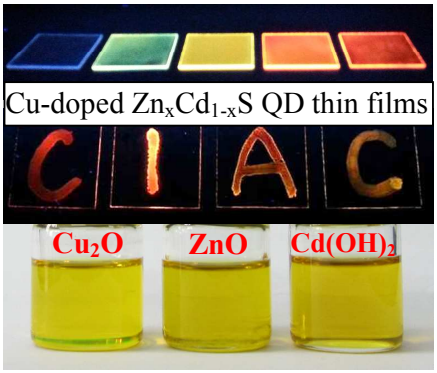

Introduction

Luminescent quantum dot thin films (QDTFs) have been extensively investigated in the past two decades due to their high potential applications in quantum dot light emitting diodes, quantum dot solar cells, thin film transistors, temperature sensors, and photodetectors.[1-15] Besides, luminescent QDTFs can absorb and covert harmful UV light to usable visible light in thin film solar cells, which can expand the photoresponse range and enhance the photoelectric conversion efficiency. Thereby, luminescent QDTFs have a high potential application in thin film solar cells. According to the reports in the literature, QDTFs are mainly fabricated by self-assembling or coating quantum dot solutions.[1-20] Thus, the synthesis of high quality quantum dots is essential. Furthermore, a ligand exchange process and a tedious post-purification procedure are usually required. These complex procedures are not suitable for highly efficient and low-cost fabrication of QDTFs. Thus, developing a direct deposition method to luminescent QDTFs without the need of the complex quantum dot synthesis using molecular-based precursor solution is of great significance.

Large-area luminescent thin films of wide-gap II-VI compounds (e.g. ZnS, ZnSe, and CdS) play an important role in visible-light optoelectronics.[21-23] ZnS with a band gap of 3.68 eV is widely used as an excellent host material for highly efficient phosphors.[24-26] Cu-doped ZnS nanocrystals are a very important class of phosphors for the fabrication of thin film electroluminescent devices. It was reported that the emission of Cu-doped ZnS QDs mainly originates from the transition from the

conduction band of ZnS to the Cu-d states.[27-30] As a result, the emission of Cu-doped ZnS QDs is strictly restricted in blue-green region.[27-30, 39] In order to achieve a tunable emission which covers the whole visible light region, Cd^{2+} ions are incorporated into the ZnS lattices to lower the conduction band position of host materials.[31-33] Although many groups have been focusing on the synthesis of Cu-doped $Zn_xCd_{1-x}S$ quantum dots, there are no reports on the direct deposition of Cu-doped $Zn_xCd_{1-x}S$ quantum dot thin film using a molecular-based precursor solution.

Here, we present a simple one-step solution approach to fabricate luminescent Cu-doped $Zn_xCd_{1-x}S$ QDTF by spin-coating a mixed Cu, Zn, and Cd precursor solution. Cu_2O, ZnO, and $Cd(OH)_2$ were used as the starting materials and dissolved in the ethanol solution of carbon disulfide and 1-butylamine, and 3-mercaptopropionic acid was used as the capping agents. All synthetic procedures were conducted in the open air. As-prepared Cu^+-doped $Zn_xCd_{1-x}S$ thin films exhibit a tunable emission covering the whole visible light region and the absolute photoluminescence quantum yield can reach as high as 25.5%.

Experimental Section

I. Chemicals.

Copper (I) oxides (Cu_2O, 99%), zinc oxide (ZnO, 99.99%), cadmium hydroxide ($Cd(OH)_2$, AR), carbon disulfide (CS_2, 99.9%), 1-butylamine ($CH_3(CH_2)_3NH_2$, 99%), ethanol (CH_3CH_2OH, AR), and 3-mercaptopropionic acid (MPA, $HSCH_2CH_2COOH$,

98%) were purchased from Aladdin. All chemicals were used as received without any further purification.

II. Preparation of Semiconductor Precursor Solution.

Zn, Cd, or Cu precursor solution (0.2 M) was prepared by dissolving 0.1628 g (2.0 mmol) of ZnO, 0.3317 g (2.0 mmol) of $Cd(OH)_2$, or 0.1430 g (1.0 mmol) of Cu_2O in 7.0 mL of ethanol, 1.2 mL of CS_2 (20 mmol), and 2.0 mL of 1-butylamine (20 mmol) under magnetic stirring on a hot plate at 60°C until all the solid dissolved, respectively. Finally, Zn, Cd, and Cu precursor solutions were mixed, followed by centrifugation at 12,000 rpm for 5 min prior to spin-coating.

III. Deposition of Cu-doped $Zn_xCd_{1-x}S$ Luminescent Thin Films.

In a typical fabrication of Cu-doped $Zn_{0.5}Cd_{0.5}S$ quantum dot thin film with a doping concentration of 1 at%, 1.0 mL of Zn stock solution, 1.0 mL of Cd stock solution, 0.02 mL of Cu stock solution, and 0.15 mL (1.7 mmol) of MPA were mixed under stirring. Luminescent Cu-doped $Zn_xCd_{1-x}S$ quantum dot thin film was spun on a coverslip (20×20×0.5 mm) at 3,000 rpm for 30 s, followed by a sintering process on a hot plate at 210 °C for 15 s in the open air. The quantum dot thin film with a thickness of ~80 nm was obtained by single spin-coating process.

VI. Characterizations.

UV-vis diffuse reflective spectra were recorded on a Shimadzu UV-3600 spectrometer. PL spectra were measured on a Hitachi F-7000 spectrophotometer equipped with a 150 W xenon lamp as the excitation source, and the PL intensity was

calculated by integration of PL curve. Absolute photoluminescence quantum yields (QYs) were measured by an absolute PL quantum yield measurement system (C9920-02, Hamamatsu Photonics K. K., Japan). The luminescence decay curve was obtained by a Lecroy Wave Runner 6100 digital oscilloscope (1 GHz) using a tunable laser (pulse width ¼ 4 ns, gate ¼ 50 ns) as the excitation source (Continuum Sunlite OPO). The powder XRD patterns were recorded using a Bruker D8 FOCUS X-ray diffractometer. The chemical composition was determined by energy disperse X-ray spectroscopy (EDS) by using a scanning electron microscope (Hitachi S-4800) equipped with a Bruker AXS XFlash detector 4010. The thickness of the thin film was measured by a step profiler (AMBIOS, XP-100). Atomic force microscope (AFM) image was taken on a Bruker Dimension Icon.

Results and Discussion

Recently, we developed a general butyldithiocarbamic acid-based molecular precursor solution approach for the fabrication of $Cu(InGa)(S,Se)_2$, $CuIn(S,Se)_2$, and $Cu_2ZnSn(S,Se)_2$ thin film solar cells with a power conversion efficiency of 8.9%, 10.1%, and 6.0%, respectively.[34-36] Thermally degradable butyldithiocarbamic acid can be *in situ* prepared by the reaction of 1-butylamine and carbon disulfide. Many types of metal oxides and hydroxides can be dissolved in butyldithiocarbamic acid, forming a variety of metal precursor solutions. Fig. 1A shows the dissolution mechanism of Cu_2O, ZnO, and $Cd(OH)_2$ in butyldithiocarbamic acid. As can be seen in Fig. 1B, the Cu, Zn, and Cd precursor solutions are clear and transparent. 3-mercaptopropionic acid was used to control the size of quantum dots in the thin

films. Cu-doped $Zn_xCd_{1-x}S$ quantum dot thin films were fabricated by spin-coating the mixed Cu, Zn, and Cd precursor solution, followed by a sintering process. By changing Zn/Cd ratios, a series of luminescent Cu-doped $Zn_xCd_{1-x}S$ quantum dot thin films were obtained, which cover the whole visible light region, as shown in Fig. 1C and Fig. 1D.

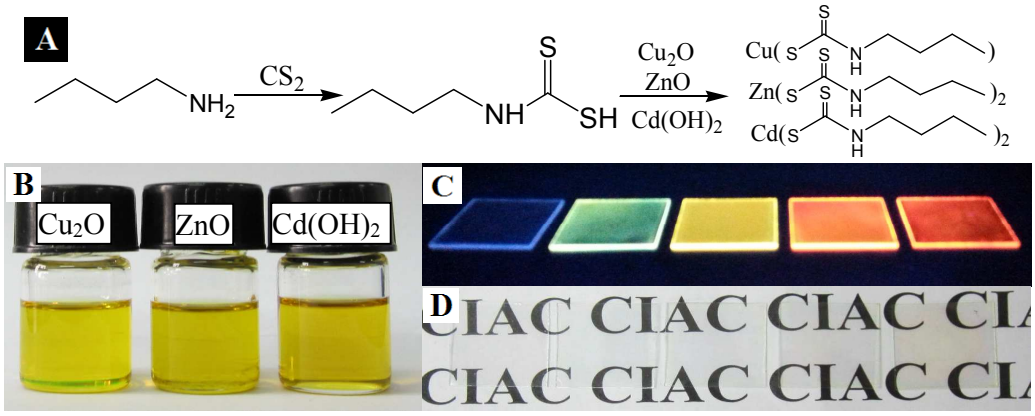

Figure 1. (A) Dissolution mechanism of Cu_2O, ZnO, and $Cd(OH)_2$ in butylamine and carbon disulfide; (B) a digital photograph of Cu, Zn, and Cd precursor solutions; digital photographs of luminescent Cu-doped $Zn_xCd_{1-x}S$ thin films with different Zn/Cd ratios under UV light irradiation (C) and under daylight illumination (D);

It was found that the photoluminescence properties of Cu-doped $Zn_xCd_{1-x}S$ quantum dot thin films are strongly influenced by Cu-doping concentration, sintering temperature, and sintering time. According to some previous reports, the dopant concentration strongly influences the PL intensity of quantum dots.[31-33] Thus, we first studied on the effect of the doping concentration on the PL intensity. Cu-doped $Zn_xCd_{1-x}S$ thin films with different Cu doping concentrations were prepared while keeping all other experimental conditions the same (e.g., molar ratio of Zn/Cd=2:1,

and the amount of MPA is 0.15 mL). Figure 2A shows several PL spectra of Cu-doped $Zn_{0.67}Cd_{0.33}S$ thin films with different Cu doping concentrations. PL intensity and peak positions of Cu-doped $Zn_{0.67}Cd_{0.33}S$ thin films show a notable dependence on the Cu doping concentration. As shown in the Fig.2B, the PL peak positions shift from 492 to 543 nm with the increasing Cu content from 0.1% to 2.0%. Interestingly, it was observed that the PL intensity of Cu-doped $Zn_xCd_{1-x}S$ thin films showed a maximum value when the Cu doping concentration is 1.0%, which is consistent with those of previously reported Cu-doped $Zn_xCd_{1-x}S$ QDs.[31-33]

In addition, the PL intensity and PL peak positions of luminescent Cu-doped $Zn_xCd_{1-x}S$ thin films are also strongly influenced by the sintering temperature (see Fig. 2C). Figure 2D illustrates the effects of the sintering temperature on the PL intensity and PL peak positions of Cu-doped $Zn_xCd_{1-x}S$ thin films. A successive red shift in PL spectra resulting from an increase of particle size was observed with increasing reaction temperature. It is well known that the final size of quantum dots is strongly dependent on the reaction temperature in a traditional wet-chemical synthesis of quantum dots. A higher reaction temperature would hinder the nucleation and result in larger quantum dots. Additionally, the PL quantum yield of quantum dots is strongly dependent on the size of quantum dots. In our system, the optimal sintering temperature was found to be 210^{o}C for the fabrication of luminescent Cu-doped $Zn_xCd_{1-x}S$ thin films.

Finally, the effect of the sintering time on the PL intensity and PL peak position was investigated, as shown in Figure 2E and 2F. The optimal sintering time was found

to be 10 s for fabricating high performance luminescent Cu-doped $Zn_xCd_{1-x}S$ thin films. Thereby, in this paper, the optimal Cu doping concentration, the sintering temperature, and the sintering time was 1.0%, 210°C, and 10 s, respectively.

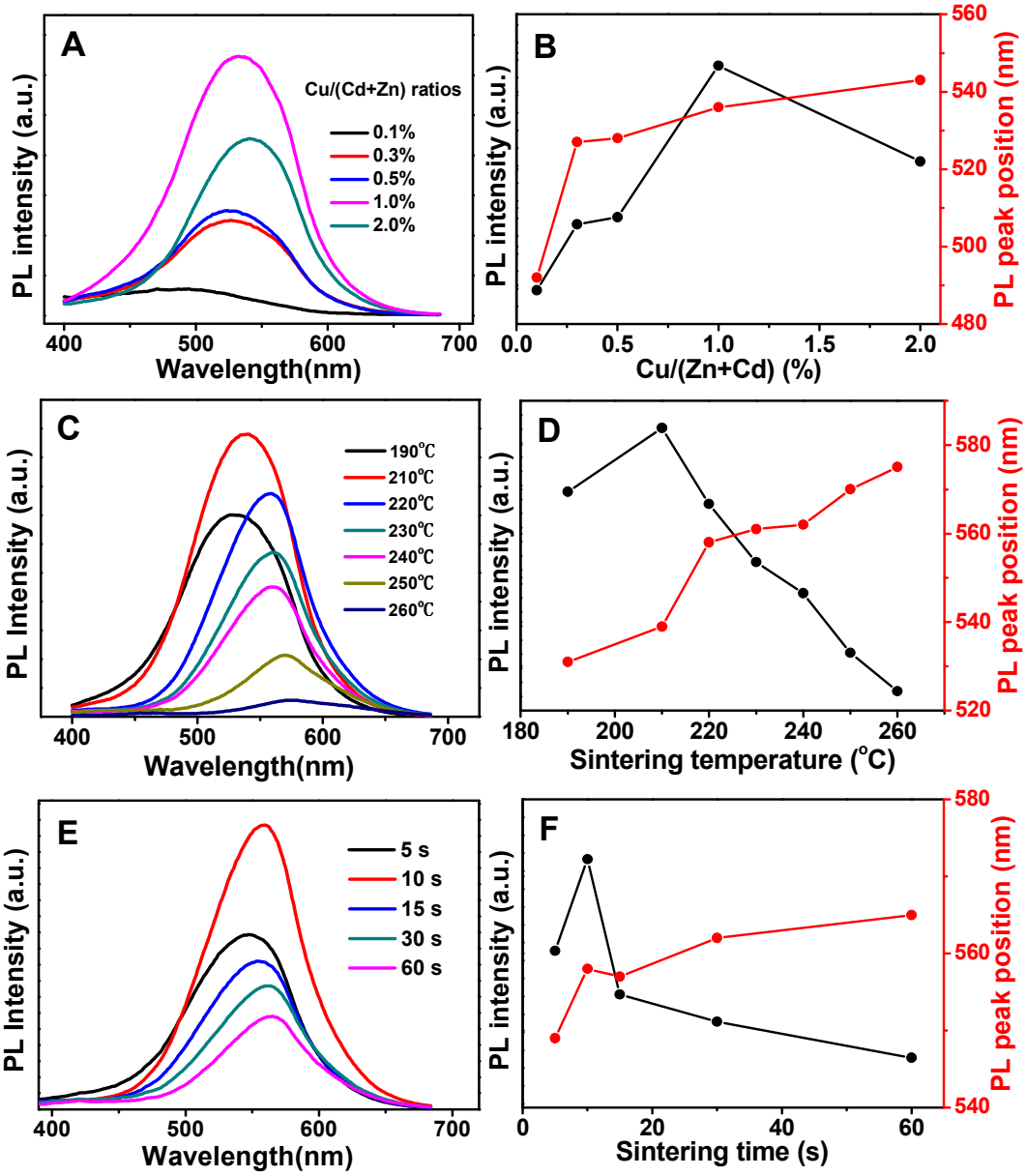

Figure 2. A series of PL spectra of Cu-doped $Zn_{0.67}Cd_{0.33}S$ thin films with different Cu-doping concentrations (A), different sintering temperatures (C), and different sintering times (E); the effects of the Cu doping concentration (B), sintering

temperature (D), and sintering time (F) on PL intensity and PL peak positions of Cu-doped $Zn_{0.67}Cd_{0.33}S$ thin films.

After the optimization of PL properties for luminescent QD thin films, Cu-doped $Zn_xCd_{1-x}S$ thin films with different Zn/Cd ratios were fabricated. The emission color of Cu-doped $Zn_xCd_{1-x}S$ thin films can be tuned by changing the molar ratio of Zn/Cd. Fig. 3A displays the UV-vis reflectance spectra of Cu-doped $Zn_xCd_{1-x}S$ films with different Zn/Cd ratios. It was reported that the band gap of Cu-doped $Zn_xCd_{1-x}S$ quantum dots was strongly related to the Zn/Cd ratio.[31-33] As expected, a successive red shift in reflectance spectra of Cu-doped $Zn_xCd_{1-x}S$ thin films was observed, as shown in Fig. 3A, confirming that a tunable band gap was obtained by changing the ratio of Zn/Cd. As a well-known phenomenon, the band gap of the alloyed $Zn_xCd_{1-x}S$ quantum dots decreases with the increase of content of low band gap CdS. Furthermore, the emission of Cu-doped $Zn_xCd_{1-x}S$ thin films originates from the transition from the conduction band of the host $Zn_xCd_{1-x}S$ to the Cu-d states. Thus, it is expected that alloyed $Zn_xCd_{1-x}S$ thin film could be a kind of host material by varying the composition to achieve a wide tunable dopant emission. With decreasing Zn/Cd molar ratio from 3:1 to 1:10, the PL spectra of Cu-doped $Zn_xCd_{1-x}S$ thin films with a tunable emission peak from 532 to 623 nm were achieved and shown in Fig. 3B. The highest absolute quantum yield of Cu-doped $Zn_xCd_{1-x}S$ thin films can reach 25.5%. In order to confirm that the emission of QD thin films does come from the transition from the conduction band to the Cu-d states, undoped $Zn_xCd_{1-x}S$ thin films with the same Zn/Cd ratios were also fabricated. Compared with pristine $Zn_xCd_{1-x}S$

thin films, the significant red-shifts in PL spectra were observed for Cu-doped $Zn_xCd_{1-x}S$ thin films (See Fig. 3C and Fig. S1), confirming that the emission of Cu-doped $Zn_xCd_{1-x}S$ thin films should be contributed to the Cu dopant state.

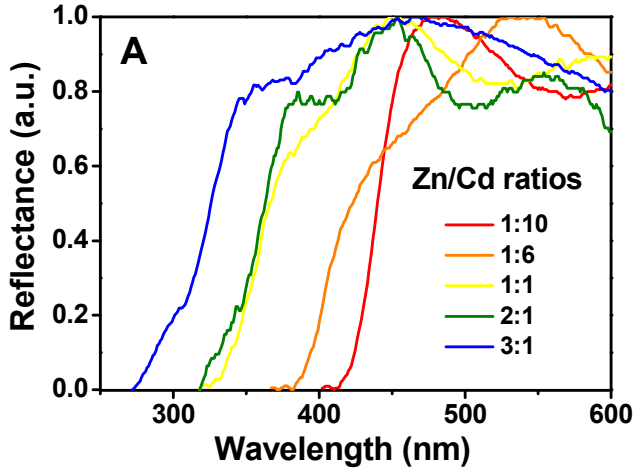

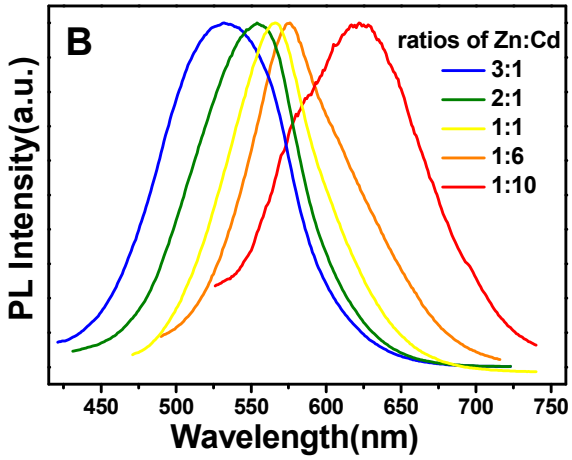

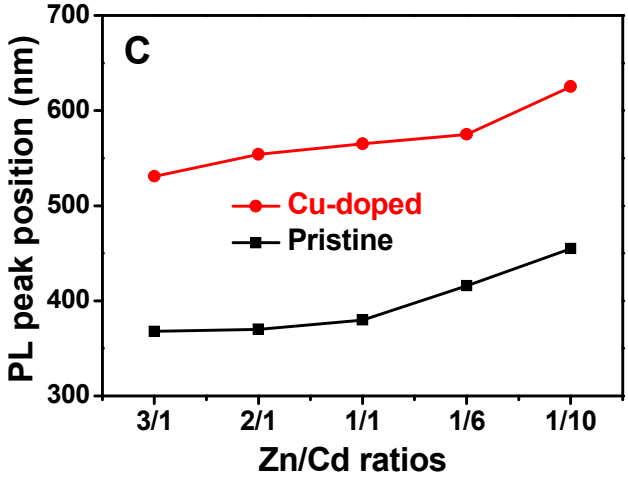

Figure 3. UV-vis reflectance spectra (A) and PL emission spectra (B) of Cu-doped $Zn_xCd_{1-x}S$ thin films with different Zn/Cd ratios; a comparison of PL peak positions for Cu-doped and pristine $Zn_xCd_{1-x}S$ thin films with different Zn/Cd ratios.

Table 1. Zn/Cd atomic ratios used in the synthesis and the real Zn/Cd atomic ratios in Cu-doped $Zn_xCd_{1-x}S$ thin films determined by EDS; the PL lifetimes and absolute PL quantum yields of Cu-doped $Zn_xCd_{1-x}S$ thin films with different Zn/Cd ratios. [a]Calculated from precursor ratios; [b]Calculated from EDS results; [c]Fast component; [d]Slow component; [e]Average PL lifetime.

Zn/Cd[a]	3:1	2:1	1:1	1:6	1:10
Zn/Cd[b]	1:0.34	1:0.52	1:0.94	1:5.88	1:9.93
Peak (nm)	543	561	572	582	615
τ_1[c] (ns)	34	21	35	10	13
τ_2[d] (ns)	277	270	327	120	175
τ[e] (ns)	251	249	291	97	151
QY (%)	16.3	17.5	25.5	24.1	18.5

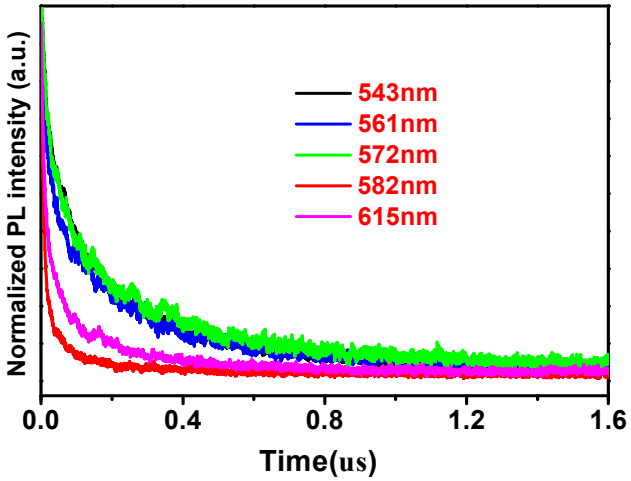

Figure 4. PL decay curves of Cu-doped $Zn_xCd_{1-x}S$ thin films with representative emission wavelengths.

The molar ratios of Zn/Cd in Cu-doped $Zn_xCd_{1-x}S$ thin films were determined by energy disperse X-ray spectroscopy (EDS), and the results were provided in Table 1. Compared with the nominal values, it was found that the real Zn/Cd ratios in samples are very close to the starting precursor ratios. In addition, the fluorescence lifetimes were measured. Figure 4 shows a series of PL decay curves of Cu-doped $Zn_xCd_{1-x}S$ thin films. The fitted PL decay data for all of the samples were listed in Table 1. All the thin films exhibit bi-exponential decays with an average fluorescence lifetime of hundreds of nanoseconds, which are in good agreement with the previous reports for Cu-doped $Zn_xCd_{1-x}S$ QDs.[21-24] Note that the fluorescence lifetimes of Cu-doped $Zn_xCd_{1-x}S$ thin films are random and independent of PL peak positions and Zn/Cd ratios.

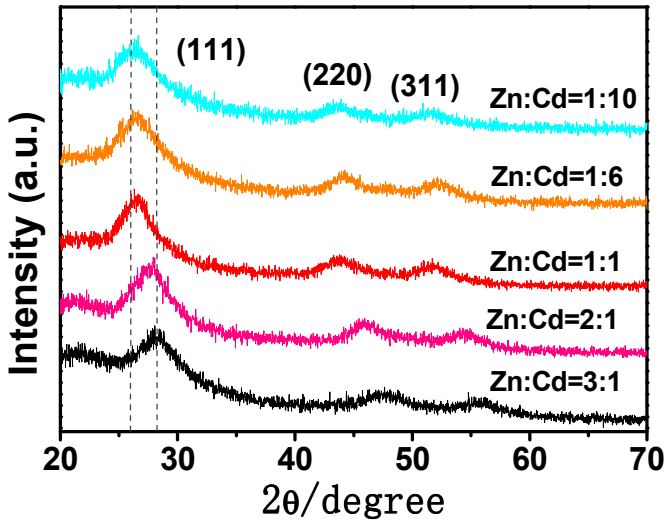

Figure 5. XRD patterns of Cu-doped $Zn_xCd_{1-x}S$ thin films with different Zn/Cd ratios.

The crystal structure of Cu-doped $Zn_xCd_{1-x}S$ thin films was measured by XRD (See Fig. 5). All of thin films exhibit three broad diffraction peaks, indicating that these

Cu-doped $Zn_xCd_{1-x}S$ thin films are composed of nanoparticles. The crystal sizes calculated by Scherrer equation are in the range of 2.2-3.6 nm, which are dependent on the Zn/Cd ratios. Detailed analysis of the XRD patterns revealed that Cu-doped $Zn_xCd_{1-x}S$ thin films have the characteristics of zincblende (ZB) structure. It was observed that the diffraction peaks systematically shift toward lower angle with increasing cadmium content in Cu-doped $Zn_xCd_{1-x}S$ thin films, indicating that the Cd^{2+} ions have been incorporated in the lattice of ZnS. It is noteworthy that the lattice mismatch between zincblende CdS and ZnS is only 7%, which enables the formation of homogeneous alloyed $Zn_xCd_{1-x}S$ thin films. Additionally, no diffraction peaks from Cu_2S and CuS impurities were detected in our samples, confirming that the incorporation of Cu ions does not result in a phase separation.

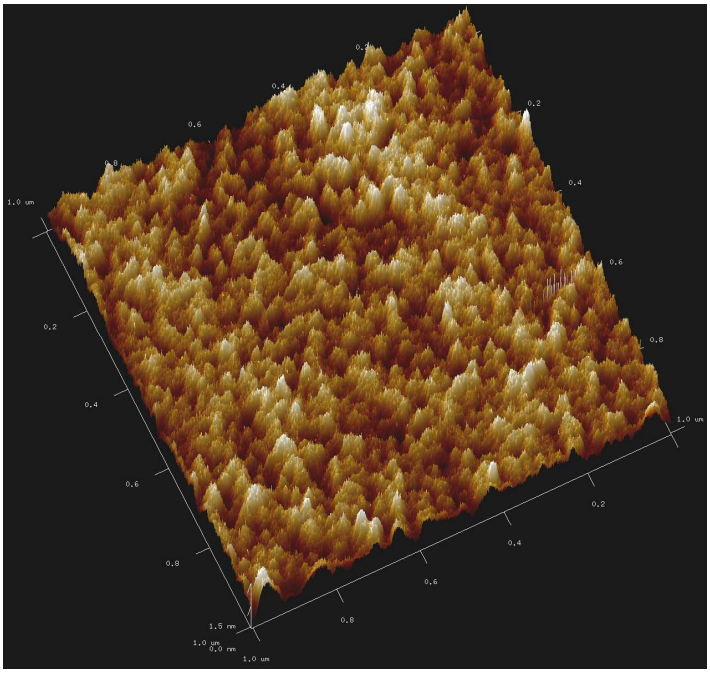

Figure 6. AFM image of Cu-doped $Zn_{0.5}Cd_{0.5}S$ quantum dot thin film.

The surface morphology and surface roughness of Cu-doped $Zn_xCd_{1-x}S$ thin film were measured by AFM. Figure 6 shows a typical AFM image of Cu-doped $Zn_{0.5}Cd_{0.5}S$ thin film. The root mean square (Rms) surface roughness of this film is 0.89 nm, which is significantly lower than those of quantum dot thin films *via* layer-by-layer assembly and spin-coating process.[14, 16] High quality quantum dot thin films are critically important to their device applications.

In thin film solar cells, UV light cannot be utilized and it is usually harmful to thin film solar cells, especially to organic solar cells and dye-sensitized solar cells since their organic components can be degraded under long-term UV light illumination.[37, 38] Thus, filtering of UV light can effectively improve the stability of thin film solar cells. Cu-doped $Zn_xCd_{1-x}S$ quantum dot thin films can absorb and convert harmful UV light to usable visible light, which can extend the photoresponse range of thin film solar cells. On the other hand, a transparent and conductive thin film is usually used as the electrode to collect the hole or electron in thin film solar cells, which impels us to fabricate luminescent, transparent, and conductive multi-functional thin films. The Cu-doped quantum dot thin films with different Zn/Cd ratios were fabricated on the opposite side of ITO layer in order to eliminate the effect of quantum dot thin films on the sheet resistance of ITO.

The absorption, excitation, and PL spectra of ITO/glass/Cu-doped $Zn_xCd_{1-x}S$ quantum dot bifacial thin films are shown in Figure 7A. It was observed that coating of Cu-doped quantum dot thin films does not significantly decrease the transmittance

of ITO layer in the wavelength range of 450 nm to 800 nm. As expected, Cu-doped $Zn_xCd_{1-x}S$ quantum dot thin films can absorb UV light and convert it to green, yellow, or red light by changing Zn/Cd ratios, as demonstrated in Figure 7B. These luminescent, transparent, and conductive multi-functional ITO/quantum dot bifacial thin films have a very high potential application in thin film solar cells. They can not only act as the UV light protection layer to improve the stability of thin film solar cells, but also can serve as the luminescent layer to convert harmful UV light to utilizable visible light.

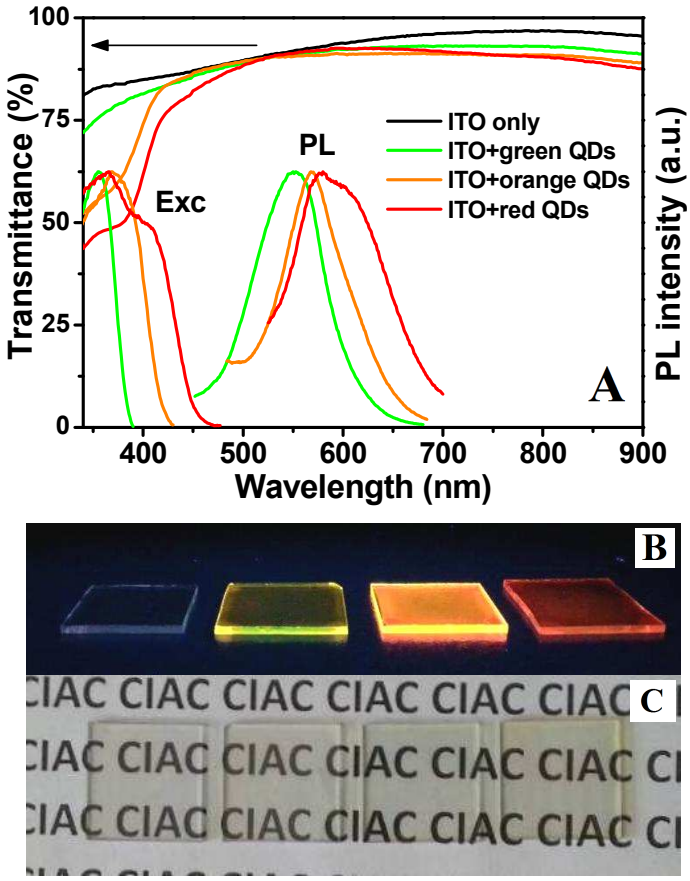

Figure 7. (A) A series of transmittance spectra, excitation spectra, and PL spectra of bifacial ITO/glass/Cu-doped $Zn_xCd_{1-x}S$ luminescent thin films with different Zn/Cd

ratios; digital photographs of bifacial ITO/glass/Cu-doped $Zn_xCd_{1-x}S$ luminescent thin films with different Zn/Cd ratios under UV light irradiation (B) and (C) under daylight illumination. The first one on the left in Fig. 7B and 7C is pure ITO glass and the other three samples are ITO/glass/QDTFs with Zn/Cd ratio of 3:1, 1:1, 1:4, respectively.

Conclusions

In summary, high quality Cu-doped $Zn_xCd_{1-x}S$ quantum dot luminescent thin films have been directly fabricated via a facile solution method using Cu_2O, ZnO, $Cd(OH)_2$, butylamine, and carbon disulfide as the starting materials. All the synthetic procedures were conducted in the open air. As-prepared luminescent thin films exhibit a tunable PL emission covering the entire visible light region by changing the Zn/Cd ratios, and the highest PL QY can reach 25.5%. The Zn/Cd ratios, the doping concentration, the sintering temperature, and the sintering time have a great effect on the PL properties of quantum dot thin films. Our experimental results indicated that luminescent quantum dot thin films have a high potential application in luminescent, transparent, and conductive thin films. More interestingly, these luminescent quantum dots thin films without the involvement of the complex quantum dot synthesis could be directly used as luminescent layer in the quantum dot light emitting diodes. The fellow-up studies are underway in our laboratory.

Acknowledgement

This work was supported by the National Natural Science Foundation of China (Grant No.91333108; 51302258; 51172229; 51202241).

Electronic supplementary information

PL spectra and EDS spectra of undoped $Zn_xCd_{1-x}S$ quantum dot thin films.

Reference

1 Z. N. Tan, F. Zhang, T. Zhu, J. Xu, A. Y. Wang, D. Dixon, L. S. Li, Q. Zhang, Mohney, S. E. Mohney and J. Ruzyllo, *Nano Lett.*, 2007, **7**, 3803.

2 P. O. Anikeeva, J. E. Halpert, M. G. Bawendi and V. Bulovic, *Nano Lett.*, 2007, **7**, 2196.

3 J. S. Stekel, S. Coe-Sullivan, V. Bulovic and M. G. Bawendi, *Adv. Mater.*, 2003, **15**, 1862.

4 Q. J. Sun, Y. A. Wang, L. S. Li, D. Y. Wang, T. Zhu, J. Xu, C. Yang and Y. F. Li, *Nat. Photonics*., 2007, **1**, 717.

5 H. S. Jang, H. Yang, S. W. Kim, J. Y. Han, S. G. Lee and D. Y. Jeon, *Adv. Mater.*, 2008, **20**, 2696.

6 J. W. Stouwdam and R. A. J. Janssen, *J. Mater. Chem*., 2008, **18**, 1889.

7 J. Tang, H. Liu, D. Zhitomirsky, S. Hoogland, X. H. Wang, M. Furukawa, L. Levina and E. H. Sargent, *Nano Lett*., 2012, **12**, 4889.

8 A. G. Pattantyus-Abraham, I. J. Kramer, A. R. Barkhouse, X. H. Wang, G. Konstantatos, R. Debnath, L. Levina, I. Raabe, M. K. Nazeeruddin, M. Gratzel and E. H. Sargent, *ACS Nano*, 2010, **4**, 3374.

9 R. Debnath, J. Tang, D. A. Barkhouse, X. H. Wang, A. G. Pattantyus-Abraham, L.

Brzozowski, L. Levina and E. H. Sargent, *J. Am. Chem. Soc*., 2010, **132**, 5952.

10 J. M. Luther, J. B. Gao, M. T. Lloyd, O. E. Semonin, M. C. Beard and A. J. Nozik, *Adv. Mater.*, 2010, **22**, 3704.

11 D. V. Talapin and C. B. Murray, *Science*, 2005, **310**, 86.

12 Y. Q. Zhang and X. A. Cao, *Nanotechnology*, 2012, **23**, 275702.

13 L. Korala, Z. J. Wang, Y. Liu, S. Maldonado and S. L. Brock, *ACS Nano*, 2013, **7**, 1215.

14 R. Z. Liang, R. Tian, W. Y. Shi, Z. H. Liu, D. P. Yan, M. Wei, D. G. Evans and X. Duan, *Chem. Comm.*, 2013, **49**, 969.

15 D. C. Oertel, M. G. Bawendi, A. C. Arango and V. Bulovic, *Appl. Phy. Lett.*, 2005, **87**, 213505.

16 F. Todescato, A. S. R. Chesman, A. Martucci, R. Signorini and J. J. Jasieniak, *Chem. Mater*., 2012, **24**, 2117.

17 O. V. Vassiltsova, S. K. Panda, Z. Y. Zhao, M. A. Carpenter and M. A. Petrukhina, *Dalton Trans*., 2009, 9426.

18 S. Chaure, N. B. Chaure and R. K. Pandey, *J. Nanosci. Nanotechno.*, 2006, **6**, 731.

19 M. K. Mishra and G. De, *J. Mater. Chem. C*, 2013, **1**, 4816.

20 I. Robel, V. Subramanian, M. Kuno and P. V. Kamat, *J. Am. Chem. Soc.*, 2006, **128**, 2385.

21 R. Maity and K. K. Chattopadhyay, *Nanotechnology*, 2004, **15**, 812.

22 T. Yao, M. Ogura, S. Matsuoka and T. Morishita, *Jpn. J. Appl. Phys.*, 1983, **22**, L144.

23 S. M. Reda, *Acta Mater.*, 2008, **56**, 259.

24 B. B. Srivastava, S. Jana, N. S. Karan, S. Paria, N. R. Jana, D. D. Sarma and N Pradhan, *J. Phys. Chem. Lett*., 2010, **1**, 1454.

25 K. Sooklal, B. Cullum, S. Angel and C. Murphy, *J. Phys. Chem.*, 1996, **100**, 4551.

26 Z. Deng, L. Tong, M. Flores, S. Lin, J. Cheng, H. Yan and Y. Liu, *J. Am. Chem. Soc.*, 2010, **133**, 5389.

27 C. Corrado, M. Hawker, G. Livingston, S. Medling, F. Bridges and Jin. Zhang, *Nanoscale*, 2010, **2**, 1213.

28 K. Manzoor, S. Vadera, N. Kumar and T. Kutty, *Mater. Chem. Phys*., 2003, **82**, 718.

29 M. Wang, L. Sun, X. Fu, C. Liao and C. Yan, *Solid State Commun.*, 2000, **115**, 493.

30 J. Huang, Y. Yang, S. Xue, B. Yang, B. Liu and J. Shen, *Appl. Phys. Lett.*, 1997, **70**, 2335.

31 Y. Chen, L. Huang, S. Li and D. Pan, *J. Mater. Chem. C*, 2013, **1**, 751.

32 W. Zhang, X. Zhou and X. Zhong, *Inorg. Chem.*, 2012, **51**, 3579.

33 B. Srivastava, S. Jana and N. Pradhan, *J. Am. Chem. Soc*., 2011, **133**, 1007.

34 G. Wang, S. Wang, Y. Cui and D. Pan, *Chem. Mater*., 2012, **24**, 3993.

35 W. Zhao, Y. Cui and D. Pan, *Energy Technol*., 2013, **1**, 131.

36 G. Wang, W. Zhao, Y. Cui, Q. Tian, S. Gao, L. Huang and D. Pan, *ACS Appl. Mater. Inter.*, 2013, **5**, 10042.

37 H. Sun, J. Weickert, H. C. Hesse and L. Schmidt-Mende, *Sol. Energy Mater. Sol. Cells*, 2011, **95**, 3450.

38 M. Carnie, T. Watson and D. Worsley, *Int. J. Photoenergy*, 2012, 506132.

39 S. Sarkar, A. K. Guria, B. K. Datra and N. Pradhan, *Nanoscale*, 2014, **6**, 3786.